Supplementary Information

$NaHCO_3$-enhanced hydrogen production from water with Fe and in-situ highly efficient and autocatalytic $NaHCO_3$ reduction into formic acid

Jia Duo,[a] Fangming Jin,*[a,b] Yuanqing Wang,*[c] Heng Zhong,[b] Lingyun Lyu,[a] Guodong Yao[a] and Zhibao Huo[a]

[a]School of Environmental Science and Engineering, State key lab of metal matrix composites, Shanghai Jiao Tong University, 800 Dongchuan Road, Shanghai 200240, China.

[b]Graduate School of Environmental Studies, Tohoku University, Aoba-ku, Sendai 980-8579, Japan.

[c]Biofunctional Catalyst Research Team, RIKEN Center for Sustainable Resource Science, 2-1 Hirosawa, Wako, Saitama 351-0198, Japan.

* E-mail: fmjin@sjtu.edu.cn; FangmingJin and Yuanqing Wang should be considered co-corresponding authors. Tel/Fax: (86) 21-54742283

Contents:

1.Experimental section.

Materials. Fe powder (325 mesh, ≥98% from Alfa Aesa; 100 mesh and 400 mesh, ≥98% Aladdin Chemical Reagent) was used in this study. $NaHCO_3$ (AR, ≥98% from Sino-pharm Chemical Reagent Co., Ltd) was used as a CO_2 resource to simplify handling. Gaseous CO_2 and H_2 (>99.995%) were purchased from Shanghai Poly-Gas Technology Co., Ltd. In this study, deionized water was used in all experiments.

Experimental Procedure. The schematic drawing of the experimental set-up have been described in detail elsewhere.[1, 2] and only a brief description is given below. The desired amount of $NaHCO_3$ (CO_2 source), reductant (Fe powder), deionized water, were loaded in a batch reactor. The reactor was made of a stainless steel 316 tubing (9.525 mm (3/8 in) o.d., 1 mm wall thickness and 120 mm length) with fittings sealed at each end, providing the inner volume of 5.7 mL. After loading, the reactor was immersed in a salt bath. During the reaction, the reactor was shaken and kept horizontally to enhance the mixture and heat transfer. After the preset reaction time, the reactor was removed from the salt bath to quench in a cold-water bath. After the reactions, the liquid, gaseous and solid samples after cooling to room temperature were collected for analysis. Water filling was defined as the ratio of the volume of the water put into the reactor to the inner volume of the reactor, and the reaction time was defined as the duration of time that the reactor was kept in the salt bath.

Product Analysis. Liquid samples were filtered (0.22 μm filter film) and then analyzed by high-performance liquid chromatography (HPLC, Aglient 1260), total organic carbon (TOC, Shimadzu TOC 5000A.), and gas chromatography/mass spectroscopy (GC/MS, Agilent 7890). The solid samples were washed with deionized water 3 times to remove impurities and ethanol 3 times to make the solid sample quickly dry. The samples were then dried in an isothermal oven at 40 °C for 3-5 hand characterized using X-ray diffraction (XRD, Shimadzu XRD-6100), Scanning Electron Microscope (SEM, FEI Quanta 200), X-ray photoelectron spectroscopy (XPS, EXCALAB 250) and Dispersive Raman Microscope (RAM, Senterra R200-L). The yield of formic acid was defined as the percentage of formic acid and the initial $NaHCO_3$ on a carbon basis. The selectivity of formic acid was defined as the ratio between the amount of carbon in formic acid and the total organic carbon in the samples by TOC analysis. The conversion of Fe is defined

as the percentage of the amount of oxidized iron divided by the initial iron atom, which was quantified by MDI jade software based on XRD patterns.

2. Analytical results of liquid and solid samples.

Liquid samples were analyzed by HPLC and GC/MS, as shown in Figure S1, the main product was formic acid. Also, analytic results from GC/MS indicated that a little acetic acid was detected. Meanwhile the peak of the solvent in the HPLC was double peak showing Figure S2. We verified that a little oxalic acid was formed by internal standard method. But the selectivity for the production of formic acid was approximately 99% by TOC analysis. These result indicated that CO_2 could be easily and high selectivity to reduce into formic acid only using Fe without any catalyst addition. So we mainly focused on the effect of the formic acid yield in our study. To study the oxidation level of Fe, solid samples after reactions were analyzed by XRD. As shown in Figure S3, the detected peaks were mainly Fe_3O_4 and Fe.

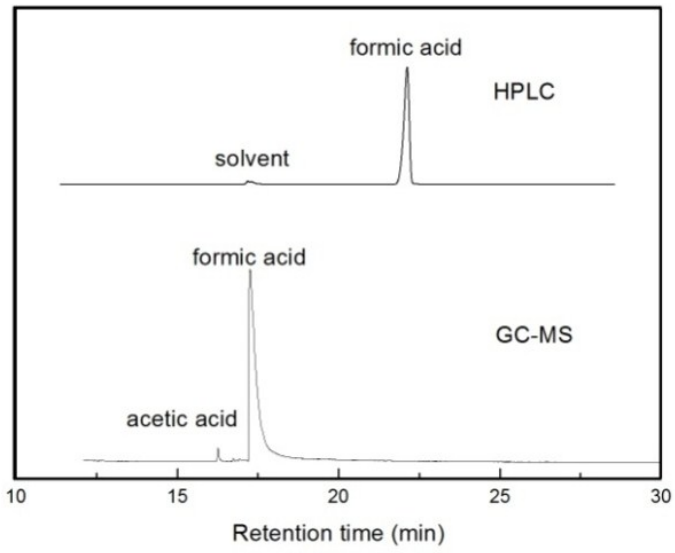

Figure S1. HPLC and GC-MS chromatogram of liquid sample after reaction (300 °C, 2 h, 2 mmol/L $NaHCO_3$, 12 mmol Fe (325 mesh), 55% water filling).

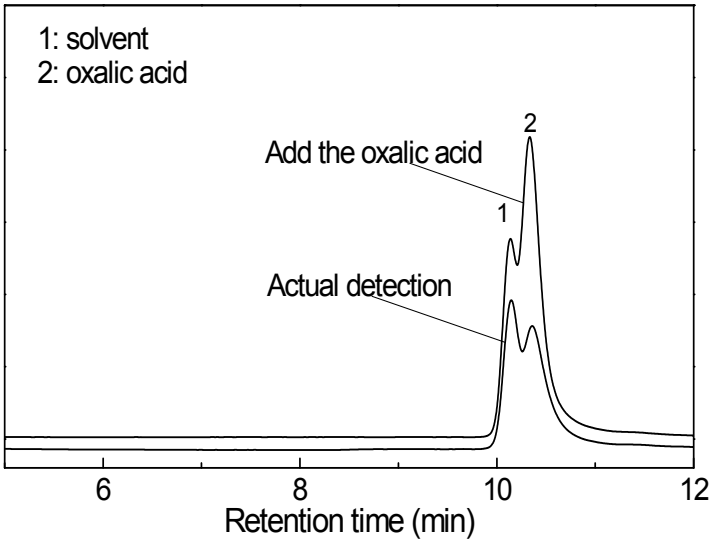

Figure S2. HPLC chromatogram at the peak of the solvent of liquid sample after reaction (300 °C, 2 h, 2 mmol/L $NaHCO_3$, 12 mmol Fe (325 mesh), 55% water filling).

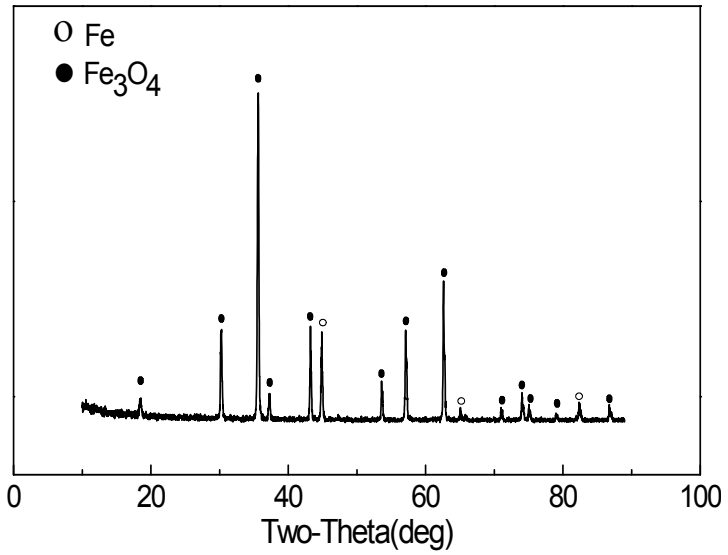

Figure S3. XRD pattern of solid residue after the reaction (300 °C, 2 h, 2 mmol/L $NaHCO_3$, 12 mmol Fe (325 mesh), 55% water filling).

3. Effect of various reaction parameters on Fe oxidation.

To enhance the oxidation of Fe, various reaction parameters were taken into account, including reaction time, temperature, the addition of NaOH and $NaHCO_3$, respectively. As shown in Table S1, among parameters investigated, $NaHCO_3$ showed better performance (entry 4).

Table S1 The conversion of Fe with the different reaction parameters

Entry	Reaction parameters	State 1	Fe Conversion（%）	State 2	Fe Conversion（%）
1	Time(min)[a]	5	73.7	120	89.4
2	Temperature(°C)[b]	275	79	325	90.6
3	NaOH(mmol)[c]	0	46.5	1	47.7
4	$NaHCO_3$ concentration (mmol/L)[d]	0.3	46.5	2	90.2

Reaction conditions: 12 mmol Fe (325 mesh), 55% water filling.

[a]300 °C, 2 mmol/L $NaHCO_3$;

[b]2 h, 2 mmol/L $NaHCO_3$;

[c]300 °C, 2 h, 0.3 mmol/L $NaHCO_3$;

[d]300 °C, 2 h.

4. Effects of $NaHCO_3$ concentration on Fe oxidation.

To test whether CO_2 could enhance the oxidation of Fe for the hydrogen production from water, experiments with Fe power in the presence and absence of $NaHCO_3$ were conducted. It was found that Fe was rarely oxidized without $NaHCO_3$, but the degree of the Fe oxidation got better in the presence of $NaHCO_3$. Thus we further changed $NaHCO_3$ to see how to effect on the oxidization of Fe. We conducted a series of experiments varying $NaHCO_3$ concentration from 0.3 to 2 mmol/L, the result showed the peak of Fe got smaller and smaller and the peak of Fe_3O_4 got stronger as the increase of $NaHCO_3$ concentration as showing Figure S4.

Then, the morphology of solid residue was examined by SEM to further verify the promotion of $NaHCO_3$ on Fe oxidation. Clearly, as shown in Figure S5, the increasing $NaHCO_3$ concentration led to the increase in the amount Fe_3O_4, and also improved the growth of Fe_3O_4 crystal to the fine grain crystal.

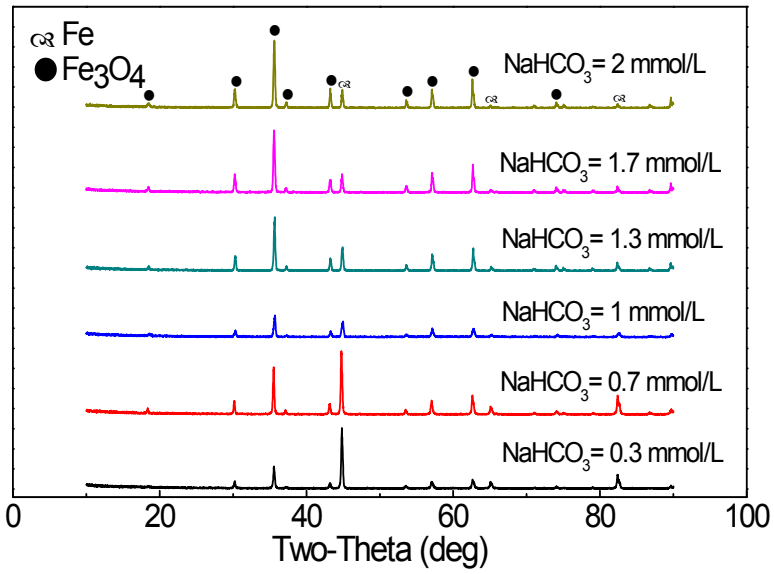

Figure S4. XRD pattern of solid residue after the reaction with the different $NaHCO_3$ concentration (300 °C, 2 h, 12 mmol Fe (325mesh), 55% water filling).

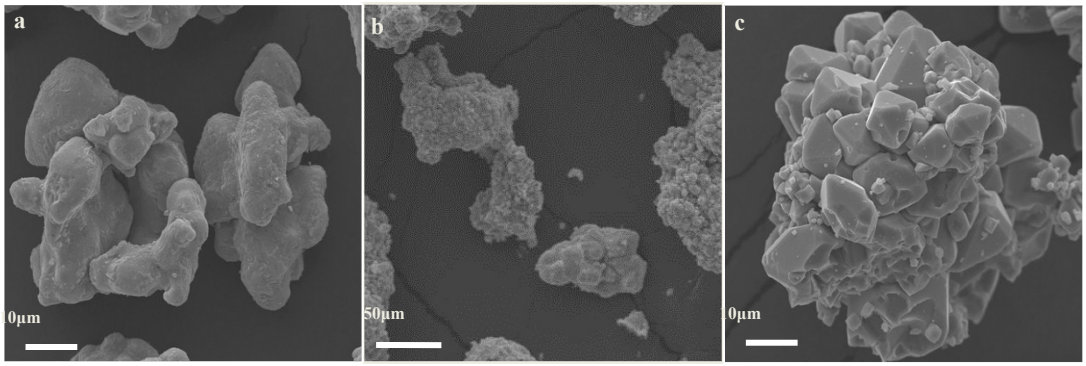

Figure S5. SEM images of the interface of solid residues with (a) 0 mmol/L $NaHCO_3$ concentration, (b) 0.3 mmol/L $NaHCO_3$ concentration and (c) 2 mmol/L $NaHCO_3$ concentration. (300 °C, 2 h, 12 mmol Fe, 55% water filling).

5. Effects of the size of Fe and water filling on the oxidation of Fe.

Subsequently, the effect of the size of Fe on the oxidation of Fe was further examined. As shown in Figure S6, Fe conversion increased first and then decreased with the decrease of the size of Fe, and the highest Fe conversion 86.3% was obtained with 325 mesh Fe power. Because the smaller size of Fe power has the lager specific area to supply active surface for the oxidation of Fe, the small size of Fe will benefit the Fe oxidation. However, Fe conversion showed a slight decrease at 400 mesh Fe power, it is probably due to the active surface that started to saturate at

400 mesh, and then slowed the Fe oxidation down.

The increase of water filling can contribute to the increase in the pressure of this system. So the experiment was conducted by changing water filling with the constant concentration of $NaHCO_3$ (1 M) to investigate the effect of the reactor pressure on the oxidation of Fe. The conversion of Fe into Fe_3O_4 firstly remained unchanged and then dropped slightly (Figure S6). It is indicated that the effect of water filling is not obvious on the oxidation of Fe.

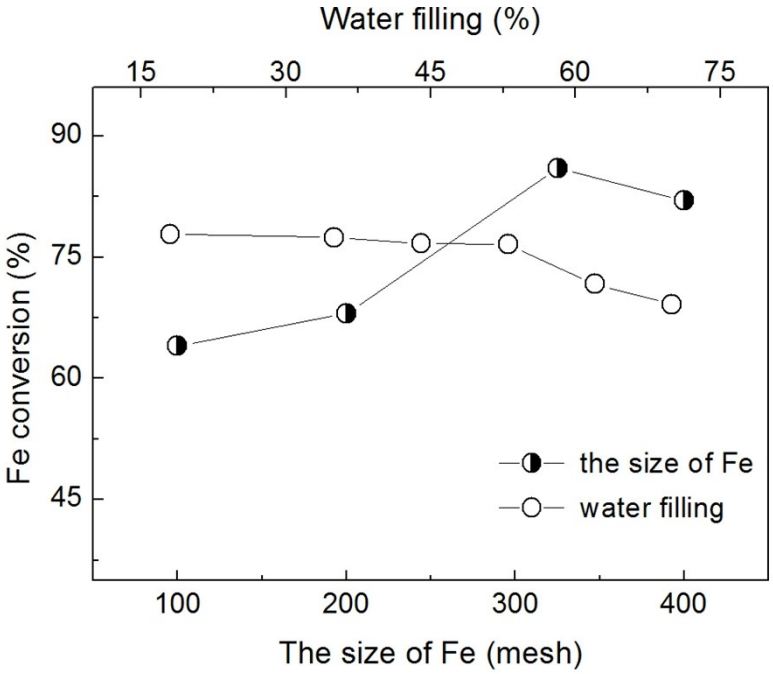

Figure S6. Effect of the size of Fe and water filling on Fe conversion (300 °C, 2 h, 12 mmol Fe; 2 mmol/L $NaHCO_3$ concentration and 55 % water filling for the size of Fe; 1 mmol/L $NaHCO_3$ concentration and 325 mesh Fe for water filling).

6. Effects of the size of Fe power on the formic acid yield.

The size of Fe power is an important factor in the oxidation of Fe, so the effect of the size of Fe powder on the formic acid yield was subsequently investigated. Firstly, 200 mesh Fe was chosen, whatever conditions to perform the yield of formic acid didn't exceeded 60%. Then we tried to investigate whether the smaller size of Fe could improve the formic acid yield, 325 mesh Fe powder was used in this experiment. As shown in Figure S7, the average amplification 10% of the yield was obtained. So we further performed the experiment of 100 mesh to 400 mesh, and the yield increased significantly from 100-325 mesh and then decreased slightly at 400 mesh (Figure

S8), which was identical with the effect on the oxidation of Fe. The smaller size of Fe power had the lager specific area to supply active surface for this reaction. Due to the drop of the formic yield was less than 5% at the size of Fe 400 mesh, according to our results, maybe the active surface started to saturate at 325 to 400 mesh and the reaction became slowly. Therefore we chose 325 mesh Fe power in the following studies.

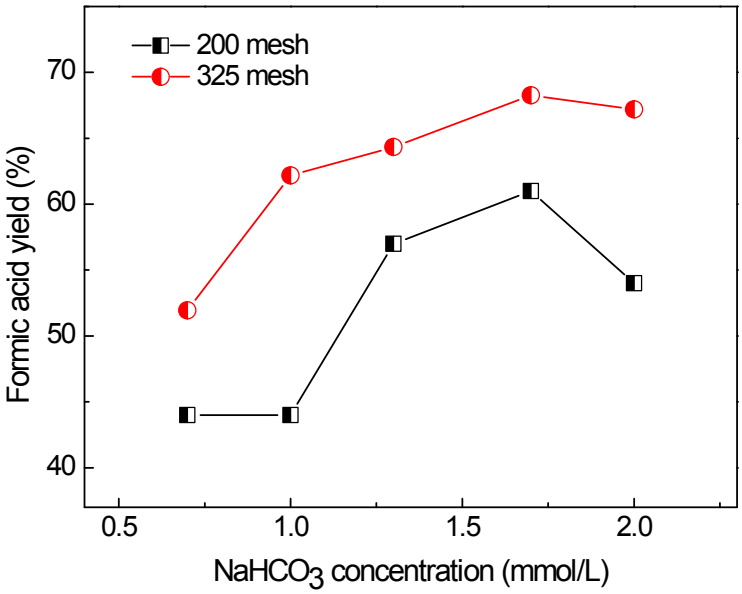

Figure S7. Effects of $NaHCO_3$ concentration with 200 mesh and 325 mesh on formic acid yield (300 °C, 2 h, 12 mmol Fe, 55% water filling).

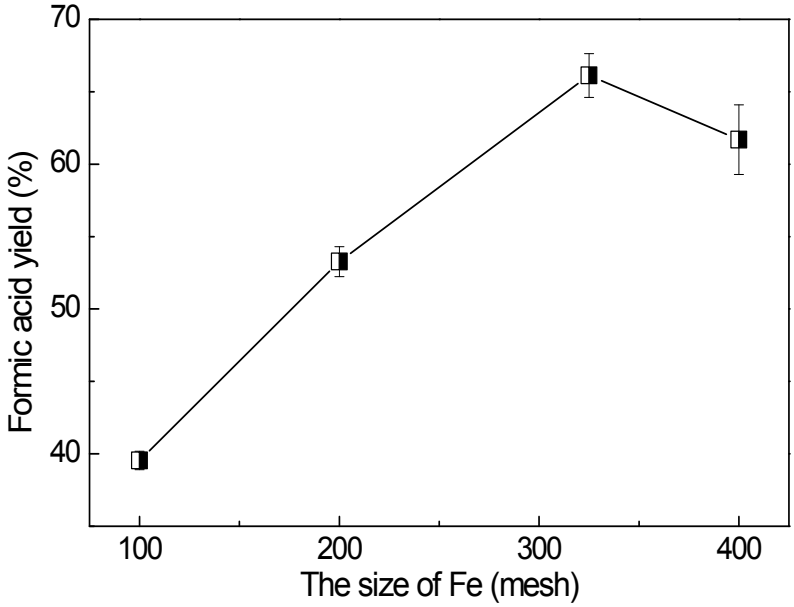

Figure S8. Effect of the size of Fe on the yield of formic acid (300 °C, 2 h, 12 mmol Fe, 55% water filling)

7. Raman scattering spectra of the oxidation product of Fe.

The distinguishing between Fe_3O_4 and γ-Fe_2O_3 phase by XRD is quite difficult because of the same inverse spinel structure and similarity in their d spacing. Hence, further precise identification of catalytic phase from iron oxides were conducted by Raman spectroscopy. As shown Figure 7, the features of Fe_3O_4 appeared at 219, 284, 399, 490 and 604 cm^{-1}, which correspond to the stretching vibration mode of Fe-O in the crystal Fe_3O_4.[3] In addition, there are not typical γ-Fe_2O_3 peaks (~700 cm^{-1}), indicating the absence of γ-Fe_2O_3.[4] These results are in agreement with the characteristic of Fe_3O_4 by XPS, which are no obvious shakeup satellite structures at the higher binding energy side of both main peaks. Therefore, the oxidation product of Fe by $NaHCO_3$ is proved to be Fe_3O_4 in our system.

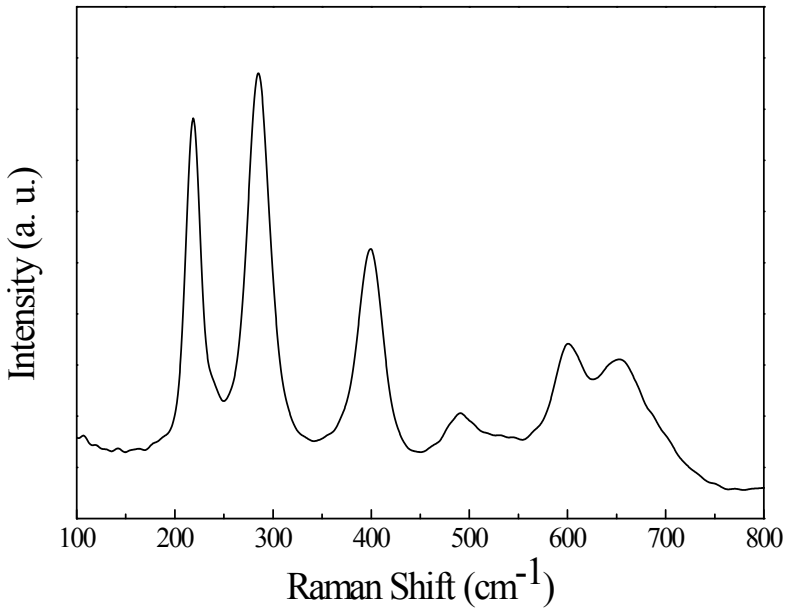

Figure S9. Raman scattering spectra of the oxidation product of Fe.

8. The proposed pathway for Fe oxidation.

According to the proposed pathway for Fe oxidation , the overall reactions of pathways can be described by:

$$Fe + 2\,NaHCO_3 + 2H_2O \rightarrow Fe(HCO_3)_2 + H_2 + 2NaOH \quad (1)$$

$$Fe(HCO_3)_2 \rightarrow FeCO_3 + CO_2 + H_2O \quad (2)$$

$$FeCO_3 \rightarrow FeO + CO_2 \quad (3)$$

$$3FeO + H_2O \rightarrow Fe_3O_4 + H_2 \quad (4)$$

9. Quantitative analysis of collected and commercial Fe_3O_4 with XPS.

Table S2 Relative intensity of Oa, Ob, and Oc peaks of the O1s spectrum of collected and commercial Fe_3O_4

	Peak binding energy (ev)			Relative intensity (%)		
	Oa	Ob	Oc	Oa	Ob	Oc
Collected Fe_3O_4	529.9	531.4	533.8	33.3	19.7	47.0
Commercial Fe_3O_4	529.7	531.3	533.2	54.7	30.6	14.8

References

1 Jin, F.; Zhou, Z.; Moriya, T.; Kishida, H.; Higashijima, H.; Enomoto, H., *Environ. Sci. Technol.* **2005,** *39*, (6), 1893-1902.

2 Jin, F.-M.; Kishita, A.; Moriya, T.; Enomoto, H., *J. Supercrit. Fluids* **2001,** *19*, (3), 251-262.

3 Oblonsky, L.; Devine, T., *Corros. Sci.* **1995,** *37*, (1), 17-41.

4 Shebanova, O. N.; Lazor, P., *J. Raman Spectrosc.* **2003,** *34*, (11), 845-852.